# Groundwater flow anomalies due to an oblate spheroid

M. Hvoždara
Geophysical Institute of the Slovak Academy of Sciences[1]

Abstract: The paper presents exact analytical solution of the potential problem of groundwater steady flow around the oblate spheroid, buried in the uniform porous medium. The diffusity coefficients of the spheroid and surrounding medium are different. The solution is expressed in the form of general spherical harmonics in oblate spheroidal co-ordinate system. The solution for unbounded medium can be also transformed into similar problem concerning the half-spheroidal (dish-like) syncline at the surface of the Earth. There is also possible calculation of the heat flow anomaly due to disturbed groundwater flow.

**Key words:** groundwater flow, potential due to spheroidal obstacle, geothermal anomalies at geosynclines

## 1. Introduction

Regardless of the progress in finite-difference or finite-element methods in solving geophysical potential problems, there are still interesting exact analytical solutions for calculation of anomalous fields due to bodies which approximate lateral inhomogeneities in the earth. One of interesting and illustrative bodies is the oblate spheroid in the unbounded space, and also half-spheroidal anomalous body at the surface of the earth.

There were presented some solutions for the D.C. geoelectric potential field *(Cook and Nostrand, 1954; Wait, 1982)*. The magnetic field anomalies can be easily calculated by the modifications of static-electricity problems treated in (*Smythe, 1968*). We shall apply similar treatment to the groundwater flow problem.

[1] Dúbravská cesta 9, 845 28 Bratislava, Slovak Republic; e-mail: geofhvoz@savba.sk

## 2. Formulation of the problem

The oblate spheroid we consider to be bounded by rotation of the ellipse with semiaxes $a, b$ ($a > b$) around the $z$ axis which prolongates the shorter semiaxis $b$ downwards to the earth. Then the section of the spheroid by horizontal plane $(x, y)$ is the circle $x^2 + y^2 = a^2$. The $(x, z)$ section of the spheroid is depicted in Fig. 1, where flow lines of the unperturbed uniform horizontal velocity field far from the spheroid are schematically depicted. Let the coefficient of filtration of the spheroid be $\kappa_T$, and in the unbounded medium $\kappa_1$. According to the steady groundwater flow theory *(Bear and Verruijt, 1987)* the velocity $\boldsymbol{V}$ of the flow is obtained as the gradient of the potential $U$:

$$\boldsymbol{V} = -\operatorname{grad} U. \tag{1}$$

The surface density of the water flow is

$$\boldsymbol{F} = \kappa \boldsymbol{V}, \quad [\boldsymbol{F}] = (\mathrm{m}^3/\mathrm{s}) \cdot \mathrm{m}^{-2} = \mathrm{m/s}. \tag{2}$$

It gives volume of the groundwater which is transported in 1 second across the $1\,\mathrm{m}^2$ area. In such treatment the filtration coefficients $\kappa_1$, $\kappa_T$ are dimensionless. The bulk volume of the fluid transported across some finite area $S$ is:

$$\Pi = \int_S \boldsymbol{F} \cdot \mathrm{d}\,\boldsymbol{S}. \tag{3}$$

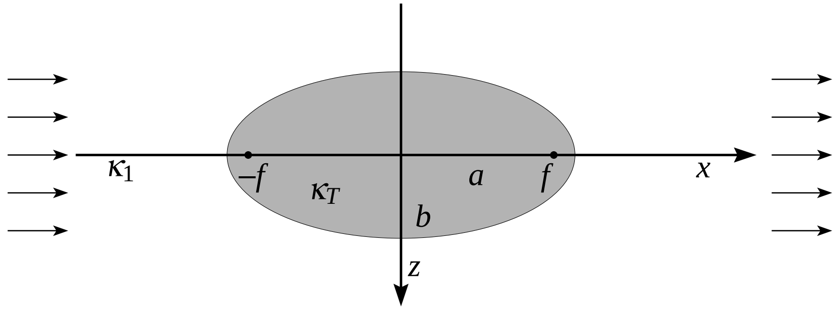


Fig. 1. The $(x, z)$ plane section of the spheroidal body (gray) in uniform unbounded space.

The velocity field $\boldsymbol{V}$ for the steady flow of the groundwater obeys the equation of continuity in the form:

$$\operatorname{div} \boldsymbol{V} = 0, \tag{4}$$

so the potential $U$ satisfies the Laplace equation:

$$\nabla^2 U = 0. \tag{5}$$

The potential of unperturbed uniform velocity field $\boldsymbol{V}_0 \equiv (V_0, 0, 0)$ far from the spheroid is:

$$U_0(x, y, z) = -V_0 \cdot x. \tag{6}$$

The presence of the spheroid causes perturbation outside the spheroid of the potential $U_1^*(x, y, z)$ which also obeys Laplace's equation:

$$\nabla^2 U_1^*(x, y, z) = 0. \tag{7}$$

The flow potential in the interior of the spheroid is $U_T(x, y, z)$, which is also the harmonic function. On the surface $\Gamma$ of the spheroid we must have continuity of the potentials and normal flow density:

$$[U_0 + U_1^*]_\Gamma = [U_T]_\Gamma\,, \tag{8}$$

$$\kappa_1 \partial \left[U_0 + U_1^*\right] / \partial n|_\Gamma = \kappa_T \left[\partial U_T / \partial n\right]_\Gamma . \tag{9}$$

The methods of mathematical physics *(Morse and Feschbach, 1953; Arfken, 1966)* give very effective tools for solutions of the above potential problem using the methods of separation of variables for the oblate spheroidal coordinate system $(\alpha, \beta, \varphi)$. These are linked to our Carthesian system $(x, y, z)$:

$$x = f \operatorname{ch} \alpha \sin \beta \cos \varphi, \quad y = f \operatorname{ch} \alpha \sin \beta \sin \varphi, \quad z = f \operatorname{sh} \alpha \cos \beta, \tag{10}$$

*(Madelung, 1957; Lebedev, 1963).* The coordinates $\alpha, \beta, \varphi$ are from intervals $\alpha \in \langle 0, +\infty)$, $\beta \in \langle 0, \pi \rangle$, $\varphi \in \langle 0, 2\pi \rangle$ and $f$ is the oblatness parameter $(f = \sqrt{a^2 - b^2})$.

From transformation equations (10) it can be derived that the coordinate surfaces $\alpha = \text{const}$ are oblate rotational ellipsoids

$$\frac{x^2 + y^2}{f^2 \operatorname{ch}^2 \alpha} + \frac{z^2}{f^2 \operatorname{sh}^2 \alpha} = 1, \quad \text{or} \quad \frac{r^2}{f^2 \operatorname{ch}^2 \alpha} + \frac{z^2}{f^2 \operatorname{sh}^2 \alpha} = 1, \tag{11}$$

where $r = \sqrt{x^2 + y^2}$ is distance from $z$ axis. The equation of generating the ellipse in the $(x, z)$ plane for our spheroid is:

$$\frac{x^2}{a^2} + \frac{z^2}{b^2} = 1. \tag{12}$$

This is matched to the spheroid $\alpha = \alpha_0$ of the sets of spheroids (11) if we put:

$$a^2 = f^2 \operatorname{ch}^2\alpha_0, \quad b^2 = f^2 \operatorname{sh}^2\alpha_0. \tag{13}$$

We know that there holds

$$\operatorname{ch}^2\alpha_0 - \operatorname{sh}^2\alpha_0 = 1, \tag{14}$$

so we easily find:

$$f^2 = a^2 - b^2, \quad f = \sqrt{a^2 - b^2}, \tag{15}$$

which means that $f$ is numerical excentricity of the generating ellipse. The polar axis for the angle $\beta$; is $z \in \langle 0, +\infty)$ it corresponds to $\beta = 0$. The coordinate surfaces $\beta = \text{const}$ are obtained from (10) by excluding $\operatorname{ch}\alpha$ and $\operatorname{sh}\alpha$ by using (14). These are confocal rotational hyperboloids (see Fig. 2):

$$\frac{r^2}{f^2 \sin^2\beta} - \frac{z^2}{f^2 \cos^2\beta} = 1. \tag{16}$$

It is necessary to note, that the plane $z = 0$ corresponds to the surface $\alpha = 0$, and the circle $x^2 + y^2 = f^2$ is the focal circle. From relations (13) we also obtain:

$$e^{\alpha_0} = (a + b)/f, \quad \alpha_0 = \ln[(a + b)/f]. \tag{17}$$

In this manner we can link spheroidal coordinate system $(\alpha, \beta, \varphi)$ with the generating ellipse. We add that Lame's metrical parameters are as follows:

$$h_\alpha = f\sqrt{\operatorname{ch}^2\alpha - \sin^2\beta}, \quad h_\beta = h_\alpha, \quad h_\varphi = f \operatorname{ch}\alpha \sin\beta, \tag{18}$$

(see e.g. Madelung, 1957). The particular solution of the Laplace equation in the system $(\alpha, \beta, \varphi)$ can be found e.g. in *(Lebedev, 1963)* in the form:

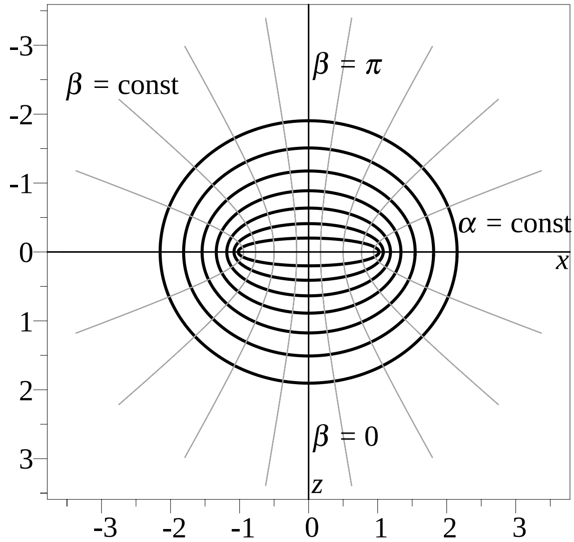


Fig. 2. The $(x, z)$ section of coordinate surfaces $\alpha$ = const (ellipses), and $\beta$ = const (hyperboles).

$$U_{mn}(\alpha, \beta, \varphi) = [M_{mn} \cos m\varphi + N_{mn} \sin m\varphi] \left\{ \begin{array}{c} P_n^m(\mathrm{i}\,\mathrm{sh}\,\alpha) \\ Q_n^m(\mathrm{i}\,\mathrm{sh}\,\alpha) \end{array} \right\} P_n^m(\cos\beta), \quad (19)$$

where $i = \sqrt{-1}$ is imaginary unit and $P_n^m(\mathrm{i}\,\mathrm{sh}\,\alpha)$, $Q_n^m(\mathrm{i}\,\mathrm{sh}\,\alpha)$ are associated Legendre functions of degree $n$, order $m$; pure imaginary argument $\mathrm{i}\,\mathrm{sh}\,\alpha$. The $P_n^m(\cos\beta)$ is known as associated Legendre function of real argument $\cos\beta$. The transformation of the unperturbed potential (6) into spheroidal system is:

$$U_0(\alpha, \beta, \varphi) = -V_0 f \,\mathrm{ch}\,\alpha \sin\beta \cos\varphi. \quad (20)$$

The dependence on $\varphi$ is given by $\cos\varphi$, so we must take in (19) the order number $m = 1$ also in potentials $U_1^*$ and $U_T(\alpha, \beta, \varphi)$. This is guaranteed by the orthogonality of goniometric functions $\cos m\varphi$ and $\sin m\varphi$ on the interval $\varphi \in \langle 0, 2\pi)$. Similarly, the dependence on $\beta$ in (20) is via $\sin\beta \equiv P_1^1(\cos\beta)$. The orthogonality of Legendre functions $P_n^m(\cos\beta)$ implicates this dependence on $\beta$ in both potential $U_1^*$ and $U_T$, so we will have the degree number $n = 1$. In the theory of general associated spherical functions *(Smythe, 1968)*, there is a proof that we can calculate it as:

$$P_1^1(\mathrm{i}\,\xi) = \sqrt{1+\xi^2}, \tag{21}$$

$$Q_1^1(\mathrm{i}\,\xi) = \frac{-\xi}{\sqrt{1+\xi^2}} + \sqrt{1+\xi^2}\,\mathrm{arctg}(1/\xi), \tag{22}$$

where we must substitute $\xi = \mathrm{sh}\,\alpha$. It can be found that $P_1^1(\mathrm{i}\,\mathrm{sh}\,\alpha^1) = (1+\mathrm{sh}^2\alpha)^{1/2} = \mathrm{ch}\,\alpha$. This function is bounded for $\alpha \to 0$, but tends to infinity for $\alpha \to \infty$. So, only this function must be used for the interior of the spheroid $\alpha \in \langle 0, \alpha_0)$. The function of the second kind $Q_1^1(\mathrm{i}\,\xi)$ has singular derivative $\mathrm{d}\,Q_1^1(\mathrm{i}\,\xi)/\partial\xi$ for $\xi = \mathrm{sh}\,\alpha \to 0$, which would give infinite gradient of potential which is physically inacceptable, since there are no sources of the field. In *(Smythe, 1968)* we can also find the more suitable expression for $Q_1^1(\mathrm{i}\,\xi)$, namely for $\xi >> 1$:

$$Q_1^1(\mathrm{i}\,\xi) = 2\sqrt{1+\xi^2}\sum_{k=0}^{\infty}\frac{(-1)^k(k+1)}{(2k+3)}\,\frac{1}{\xi^{2k+3}}. \tag{23}$$

It is clear that $\lim_{\alpha\to\infty} Q_1^1(\mathrm{i}\,\mathrm{sh}\,\alpha) = 0.$

In view of the properties $P_1^1(\mathrm{i}\,\mathrm{sh}\,\alpha)$ and $Q_1^1(\mathrm{i}\,\mathrm{sh}\,\alpha)$ the potential in the interior of the spheroid will be:

$$U_T(\alpha,\beta,\varphi) = -V_0 B_1 f\,\mathrm{ch}\,\alpha\sin\beta\cos\varphi. \tag{24}$$

The perturbing potential outside of the spheroid will be:

$$U_1^*(\alpha,\beta,\varphi) = -V_0 f A_1 Q_1^1(\mathrm{i}\,\mathrm{sh}\,\alpha)\sin\beta\cos\varphi, \tag{25}$$

since $P_1^1(\cos\beta) = \sin\beta$. The total potential outside of spheroid is:

$$U_1(\alpha,\beta,\varphi) = -V_0 f\left[\mathrm{ch}\,\alpha + A_1 Q_1^1(\mathrm{i}\,\mathrm{sh}\,\alpha)\right]\sin\beta\cos\varphi. \tag{26}$$

The coefficients $A_1 B_1$ which determine the change of the potentials of the velocity are determined from boundary conditions on the surface of the spheroid, where $\alpha = \alpha_0$ and $\kappa\partial U/\partial n = \kappa\boldsymbol{n}_\alpha\cdot\mathrm{grad}\,U = \kappa h_\alpha^{-1}\partial U/\partial\alpha$. Then the boundary conditions (8), (9) are transformed into the form:

$$[U_T]_{\alpha_0} = [U_1]_{\alpha_0}, \tag{27}$$

$$\kappa_T \left[\partial U_T/\partial\alpha\right]_{\alpha 0} = \kappa_1 \left[\partial U_1/\partial\alpha\right]_{\alpha 0}. \tag{28}$$

After substituting (24) and (26) taking into account the continuity of surface harmonics $\sin\beta\cos\varphi$, we obtain two linear equations for $A_1, B_1$:

$$\begin{aligned} &\operatorname{ch}\alpha_0 + A_1 Q_1^1(\mathrm{i}\operatorname{sh}\alpha_0) = B_1 \operatorname{ch}\alpha_0, \\ &\operatorname{sh}\alpha_0 + A_1\,\mathrm{i}\operatorname{ch}\alpha_0 Q_1^{1\prime}(\mathrm{i}\operatorname{sh}\alpha_0) = (\kappa_T/\kappa_1) B_1 \operatorname{sh}\alpha_0. \end{aligned} \tag{29}$$

The solution will give:

$$A_1 = \frac{(\kappa_T/\kappa_1 - 1)\operatorname{sh}\alpha_0\operatorname{ch}\alpha_0}{\mathrm{i}(\operatorname{ch}\alpha_0)^2 Q_1^{1\prime}(\mathrm{i}\operatorname{sh}\alpha_0) - (\kappa_T/\kappa_1)\operatorname{sh}\alpha_0 Q_1^1(\mathrm{i}\operatorname{sh}\alpha_0)}, \tag{30}$$

$$B_1 = 1 + A_1 Q_1^1(\mathrm{i}\operatorname{sh}\alpha_0)/\operatorname{ch}\alpha_0. \tag{31}$$

In this manner we can calculate the necessary potentials and their gradients velocity field.

## 3. Numerical calculations for the spheroid in unbounded medium

Now we pay our attention to the calculations of the potential and velocity field in Carthesian coordinates. The expression (24) of the interior potential can be easily transformed, since according to (10) we have $x = f\operatorname{ch}\alpha\sin\beta\cos\varphi$. Then:

$$U_T(x, y, z) = -V_0 B_1 \cdot x. \tag{32}$$

It corresponds to the uniform, $x$-oriented velocity field $\boldsymbol{V}_T \equiv (V_0 \cdot B_1, 0, 0)$ in the Carthesian system. The potential $U_1(\alpha, \beta, \varphi)$ outside of the spheroid is the sum of the unperturbed potential $U_0(\alpha, \beta, \varphi)$ and the perturbing potential $U_1^*(\alpha, \beta, \varphi)$. We wish to calculate this perturbing potential and its gradient in a network of $(x, y, z)$ variables, so we must calculate proper spheroidal coordinates $(\alpha, \beta, \varphi)$. We can calculate the values of $\operatorname{ch}\alpha, \operatorname{sh}\alpha$ by using the transformation relations (10) and the properties of confocal ellipses. We know that the coordinate line $\alpha = \text{const}$ is an ellipse of equation (11) in $(r, z)$ plane; their foci are in points $r = \pm f$ in the plane $z = 0$, major semiaxis is $f\operatorname{ch}\alpha$ and minor semiaxis is $f\operatorname{sh}\alpha$. For every $(r, z)$ point of this ellipse it is the sum of distances from the first and second focus equal to the doubled value of major semiaxis which is $2f\operatorname{ch}\alpha$. There must hold:

$$\left[(r-f)^2+z^2\right]^{1/2}+\left[(r+f)^2+z^2\right]^{1/2}=2f\,\mathrm{ch}\,\alpha, \tag{33}$$

where $r=\sqrt{x^2+y^2}$. From this equation we can determine the value $\mathrm{ch}\,\alpha$, since $f=\sqrt{a^2-b^2}$ is a constant given by the contour ellipse of the spheroid which creates whole family of confocal ellipses $\alpha=\mathrm{const}$. From known value of $\mathrm{ch}\,\alpha$ we can determine $\mathrm{sh}\,\alpha$ as

$$\mathrm{sh}\,\alpha=\left[\mathrm{ch}^2\alpha-1\right]^{1/2}, \tag{34}$$

$$\text{and}\quad e^{\alpha}=\mathrm{ch}\,\alpha+\mathrm{sh}\,\alpha. \tag{35}$$

Then we can easily determine also the value of coordinate $\beta$, using (10), which gives:

$$\cos\beta=z/(f\,\mathrm{sh}\,\alpha) \tag{36}$$

for $z=0$ and $r>f$ these relation holds also true (there we have $\mathrm{ch}\,\alpha=r/f$ and $\beta=\pi/2$). Inside of focal circle $z=0$, $r<f$ we must be more careful. The value of $\alpha$ is zero and from (33) we have:

$$2f\,\mathrm{ch}\,\alpha=|r-f|+|r+f|=f-r+r+f=2f, \tag{37}$$

so we obtain $\mathrm{ch}\,\alpha=1$, $\mathrm{sh}\,\alpha=0$. But inside this circle the value of coordinate $\beta$ is changing as follows from the equation of confocal hyperboloids (16), where we put $z=0$ an then

$$\sin\beta=r/f. \tag{38}$$

For the azimuthal angle $\varphi$ we have:

$$\mathrm{tg}\,\varphi=y/x. \tag{39}$$

Using these formulae we can assign to each $x,y,z$ point its spheroidal coordinates $(\alpha,\beta,\varphi)$ and calculate the perturbing potential:

$$U_1^*(\alpha,\beta,\varphi)=-V_0\,f\,A_1Q_1^1(\mathrm{i}\,\mathrm{sh}\,\alpha)\sin\beta\cos\varphi, \tag{40}$$

and also components of the velocity:

$$\boldsymbol{V}^*(\alpha,\beta,\varphi)=-\,\mathrm{grad}\,U_1^*(\alpha,\beta,\varphi),$$

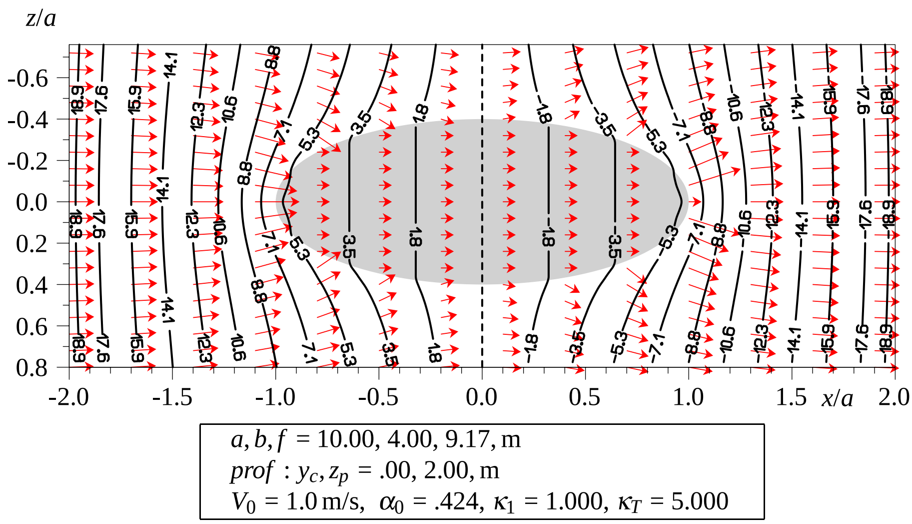


Fig. 3a. Equipotential lines $U(x, 0, z)$ in $[\mathrm{m}^2/\mathrm{s}]$, (full lines) and velocity arrows inside and around the spheroid for $\kappa_T/\kappa_1 = 5$.

$$V_\alpha^* = -\frac{1}{h_\alpha}\frac{\partial U_1^*}{\partial \alpha}, \quad V_\beta^* = -\frac{1}{h_\beta}\frac{\partial U_1^*}{\partial \beta}, \quad V_\varphi^* = -\frac{1}{h_\varphi}\frac{\partial U_1^*}{\partial \varphi}. \tag{41}$$

These derivatives can be easily calculated, but we need to transform these spheroidal vector components into Carthesian ones. We can use the relations given in *(Madelung, 1957)* with proper changes of the spheroidal coordinates notation:

$$\begin{aligned}
V_x^* &= V_r^* \cos\varphi - V_\varphi^* \sin\varphi, \\
V_y^* &= V_r^* \sin\varphi - V_\varphi^* \cos\varphi, \\
V_z^* &= \left[-V_\beta^* \sin\beta \,\mathrm{sh}\,\alpha + V_\alpha^* \,\mathrm{ch}\,\alpha \cos\beta\right] \cdot \left[\mathrm{ch}^2\alpha - \sin^2\beta\right]^{-1/2},
\end{aligned} \tag{42}$$

where

$$V_r^* = \left[-V_\alpha^* \sin\beta \,\mathrm{sh}\,\alpha + V_\beta^* \,\mathrm{ch}\,\alpha \cos\beta\right] \cdot \left[\mathrm{ch}^2\alpha - \sin^2\beta\right]^{-1/2}$$

is the radial velocity component in $x, y$ plane.

For our numerical calculations have chosen various parameters of the spheroid. In order to reduce the number of figures we present here isoline

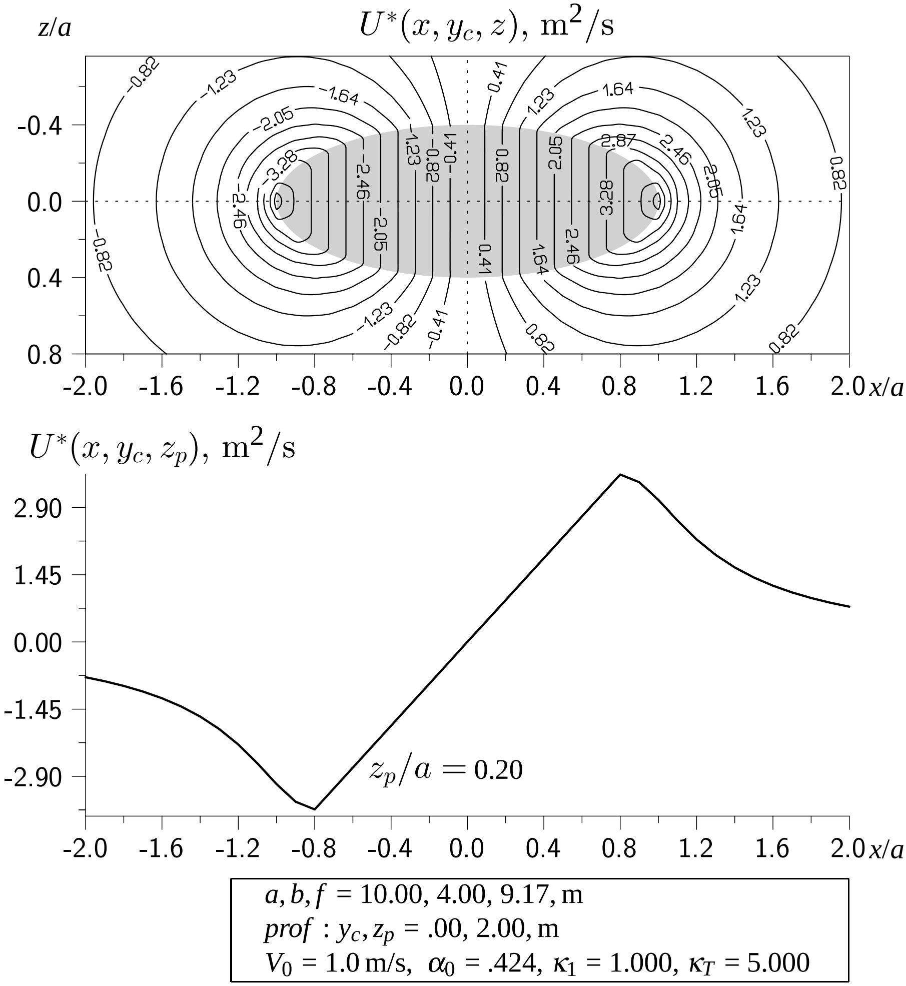


Fig. 3b. The equipotential lines of the perturbing potential $U^*(x, y_c, z)$ in [m$^2$/s], inside and around the spheroid for $\kappa_T/\kappa_1 = 5$, and its profile curve for $z_p/a = 0.2$.

and profile curves for the spheroid with dimensions $a = 10\,\text{m}$, $b = 4\,\text{m}$, which gives $f = (a^2 - b^2)^{1/2} = 9.165\,\text{m}$ and the parameter $\alpha_0$ according to (17) is $\alpha_0 = 0.424$. We put filtration ratio $\kappa_T/\kappa_1 = 5$, which means that the spheroidal body is highly porous (penetrable) in comparison with the surrounding medium. We put the unperturbed velocity $V_0 = 1\,\text{m/s}$,

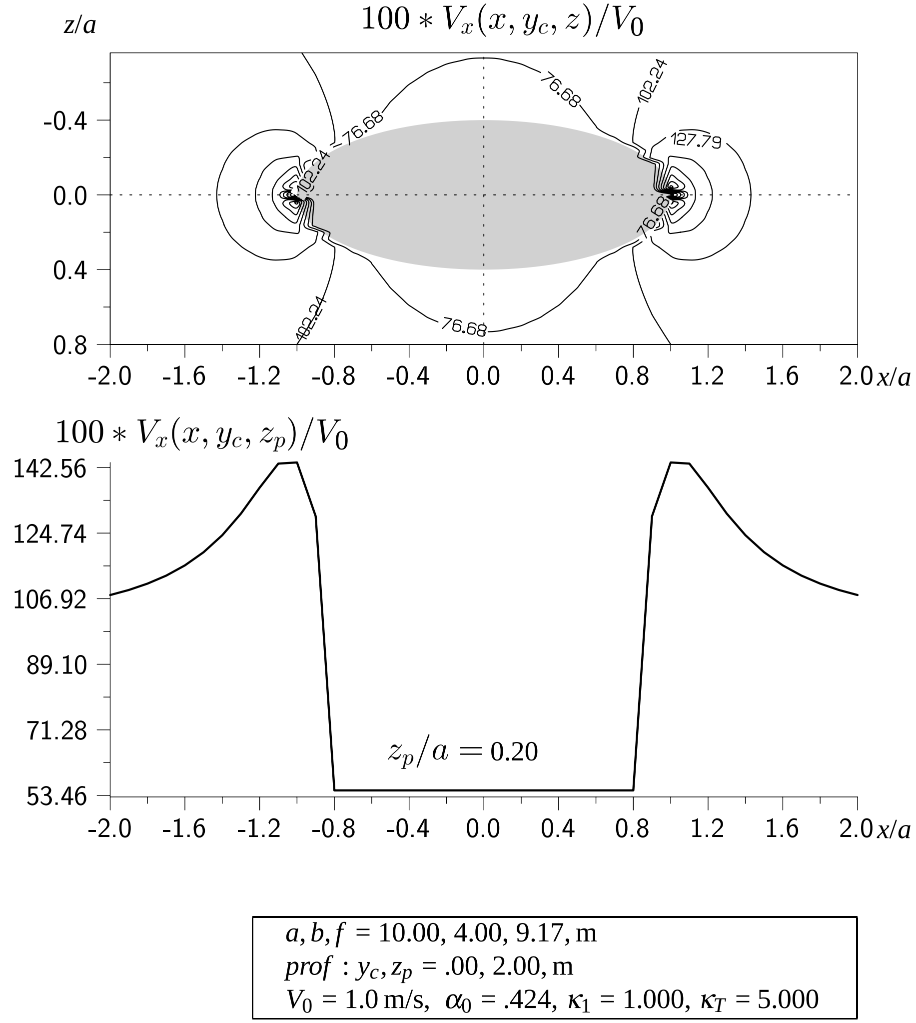


Fig. 3c. The isolines of the horizontal $V_x$-component of the flow velocity, inside and around the high porosive spheroid $\kappa_T/\kappa_1 = 5$. The profile curve shows more detailed course of $V_x$ along the line $y_c = 0$, $z_p/a = 0.2$.

which is unusually high for real groundwater, but the presented results can be easily matched to smaller values of $V_0$, e.g. $V_0 = 0.01\,\mathrm{m/s}$. In series of Figs. 3a–d we present isoline results for the central plane $y_c = 0$, and profile

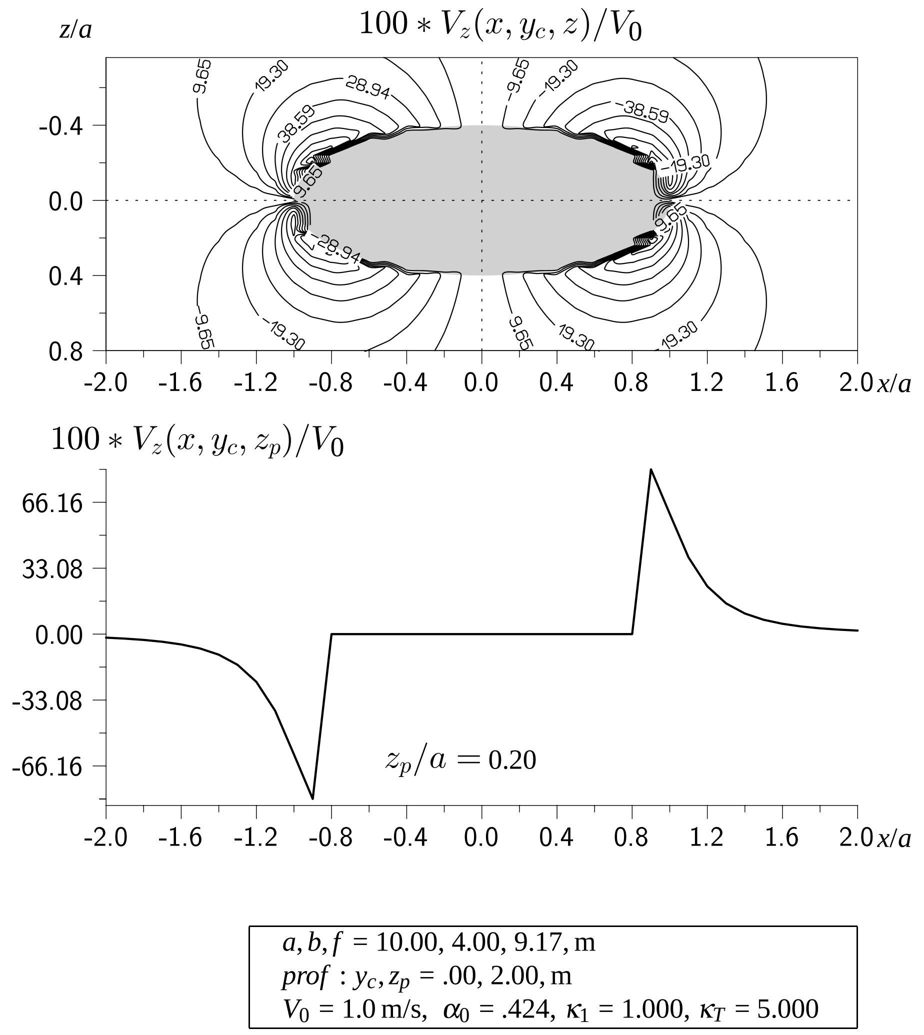


Fig. 3d. The same as in Fig. 3c, but for the vertical component $V_z$.

curves are plotted for the depth $z_p = b/2$ (2 m), which corresponds to some $z$-shifted plane in the spheroid. In Fig. 3a we can see isolines of total potential $U(x, 0, z)$ around and inside of spheroid (full lines), and vector around the velocity field (gray arrows). The length of velocity arrows was restricted to some interval, but their directions are true. We can see that far from

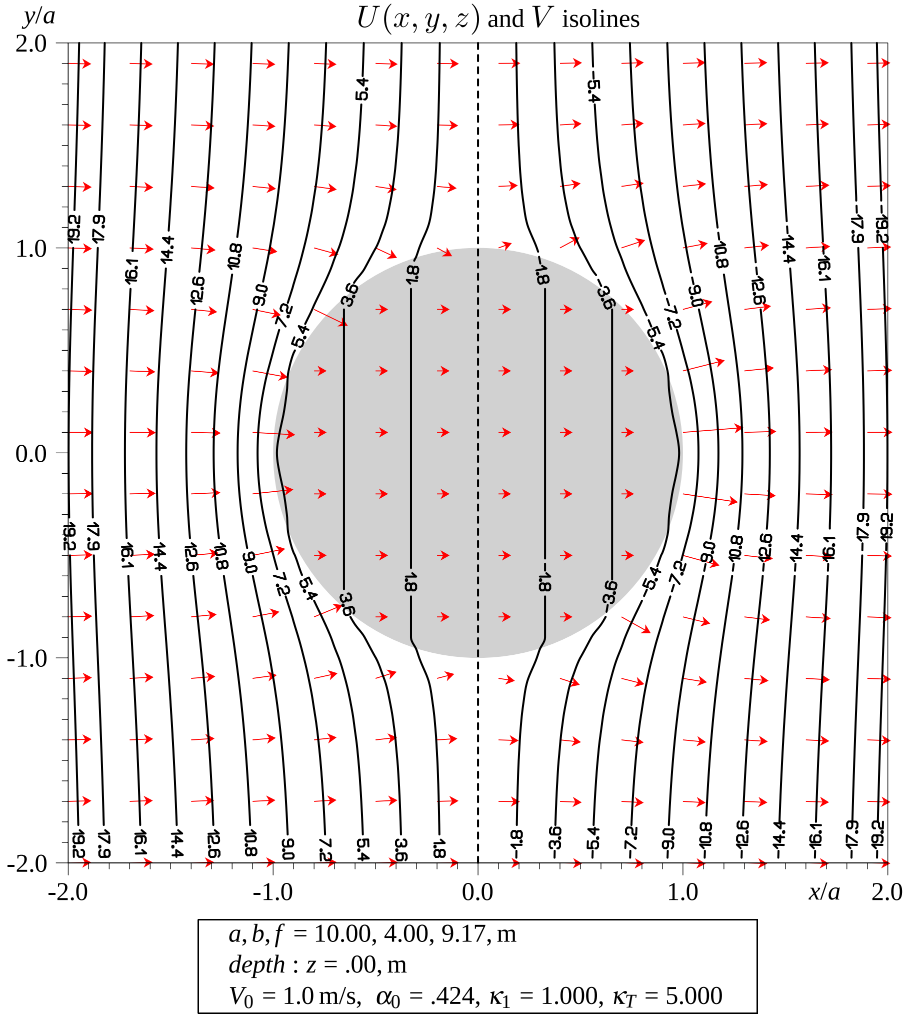


Fig. 4a. Equipotential lines $U(x,y,0)$ in [m$^2$/s], (full lines) and velocity arrows inside and around the spheroid for $\kappa_T/\kappa_1 = 5$. The gray circle is the cross-section of the spheroid by the plane $z = 0$.

the spheroid there is velocity field uniform, $x$-directed, but the spheroid with high filtration coefficient $(\kappa_T/\kappa_1) = 5$ attracts the velocity arrows to its surface. Inside of the spheroid the velocity field is again uniform, and

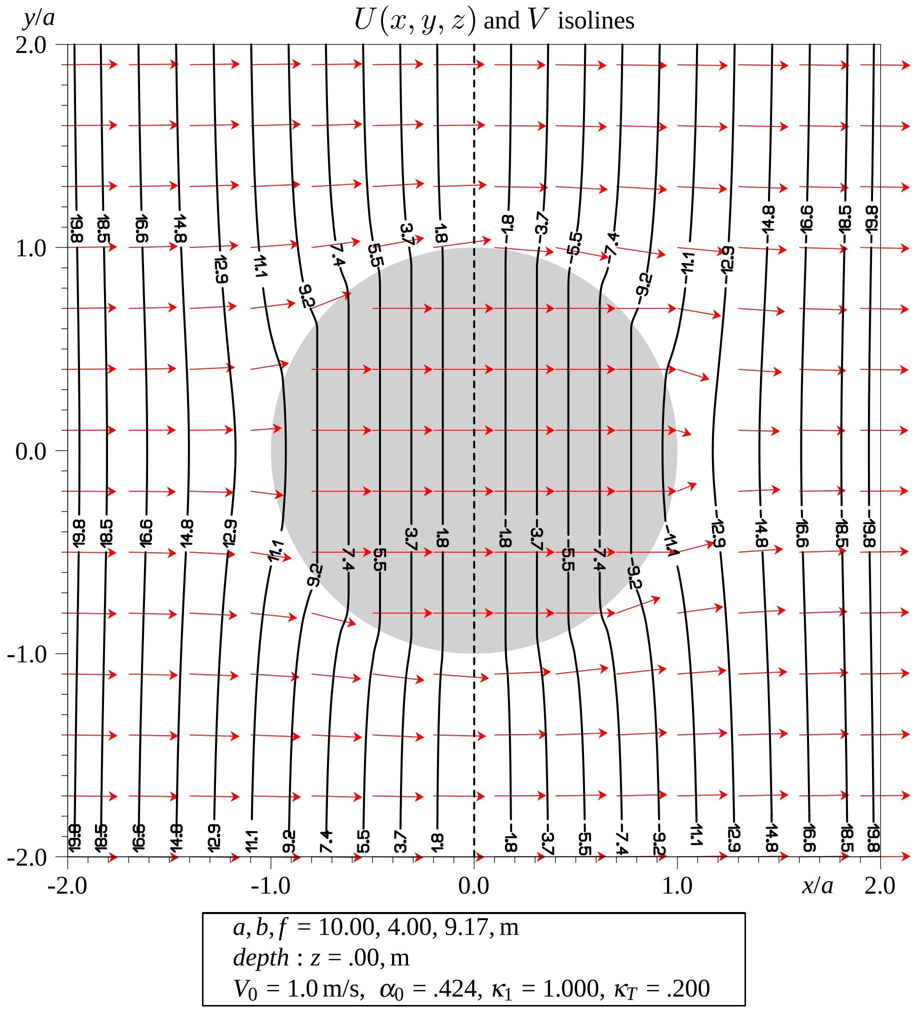


Fig. 4b. The same as in Fig. 4a, but for the spheroid with $\kappa_T/\kappa_1 = 0.2$.

$x$-directed in agreement with potential (32). Although the velocity values inside of the spheroid are low (shown in Fig. 3b), the continuity of normal flow on the spheroid boundary is preserved according the boundary condition (28). In Fig. 3b we present isolines of anomalous potential $U^*$ in the central plane ($y_c = 0$) inside and around the spheroid, and in addition its

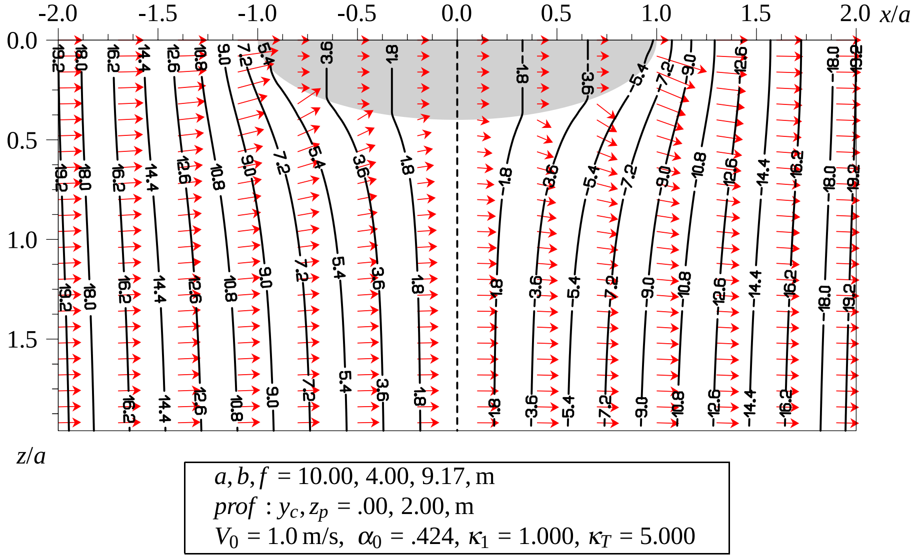


Fig. 5a. Equipotential lines $U(x, 0, z)$ in [m$^2$/s], (full lines) and velocity arrows inside and around the half spheroid for $\kappa_T/\kappa_1 = 5$.

profile curve along the line $y_c = 0$, $z_p/a = 0.2$. Figs. 3c and 3d present calculated values of $V_x/V_0$, and $V_z/V_0$ in isoline maps and also along the selected profile line mentioned above. The $V_y$ component of velocity is not presented, since it is zero in all the plane $y_c = 0$. Note, that $V_z$ is zero inside of the spheroid, since grad $U_T$ has zero value of its $z$-component, as follows from the formula (32). The $V_x$ values are also decreased inside the spheroid because of high $\kappa_T/\kappa_1$ value, but the continuity of normal water flow $\boldsymbol{n} \cdot \boldsymbol{F}$ on the surface of spheroid is preserved. In order to study the velocity field in the plane $z = 0$ we present Figs. 4a,b for two cases of $\kappa_T/\kappa_1 = 5$ or 0.2. We can see total potential isolines and also directions of the flow in horizontal $x, y$ plane, where the cross-section of the spheroid is the circle of radius $a$. When $\kappa_T/\kappa_1 = 5$, the velocity lines tend to flow into high porous spheroid (Fig. 4a), but if $\kappa_T/\kappa_1 = 0.2$, they avoid this region.

The solution of our problem can be easily used as a solution for the half-spheroidal body (syncline) at the surface of the earth. On the planar surface $z = 0$ we must have zero value of vertical velocity component. This boundary condition is guaranteed by the property $[\partial U/\partial z]_{z=0} = 0$,

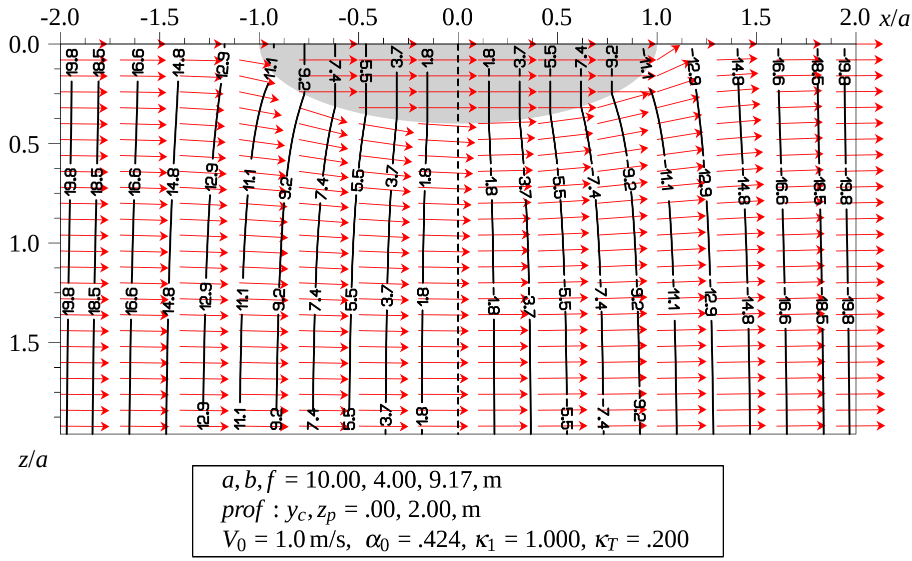


Fig. 5b. Equipotential lines $U(x, 0, z)$ in $[\mathrm{m}^2/\mathrm{s}]$, (full lines) and velocity arrows inside and around the half spheroid for $\kappa_T/\kappa_1 = 0.2$.

which is satisfied, because the potentials $U_0, U_1^*(\alpha, \beta\varphi)$, $U_T(\alpha, \beta, \varphi)$ satisfy the boundary condition $h_\beta^{-1} \left[\partial U/\partial\beta\right]_{\beta=\pi/2} = 0$. Their $\beta$-dependence is via $\sin\beta$ and surface $\beta = \pi/2$ is identical with $z = 0$, where $\mathrm{d}\sin\beta/\,\mathrm{d}\,\beta = 0$. According to formulae (42) the perturbation part of velocity $V_z^*$ attains zero value clearly, because $V_\alpha^*$ is multiplied by $\cos\beta$. Figures 5a,b show potential lines and velocity arrows for the $y_c = 0$ for both ratios of $\kappa_T/\kappa_1$ (=5 or 0.2). Comparing the part $z > 0$ of Fig. 3a with 5a we see their identity.

For the geothermal water flow we can also obtain some knowledge in a similar way as in our previous paper *(Hvoždara, 2005)* for the cylindrical obstacle in the halfspace. It has been proved that the convective heat transfer is controlled by the vertical component of velocity, the heat flow density is $q_{cn} = -C_v\rho T V_z$, where $C_v$ is the specific volume heat, $\rho$ is the water density, $T$ is temperature. The negative sign in this formula is due to our orientation of $z$-axis, down into earth. Although we did not calculate some model for the temperature perturbation due to the spheroid, we can obtain some qualitative results considering the groundwater flow velocity field. From Fig. 3d we can see that the convective heat transport to the earth's surface is positive in the region outside of the left quarter of the spheroid ($x < 0, z > 0$), where $V_z$ is negative. The profile curve for the depth $z_p/a = 0.2$ shows that the disturbance in $V_z$ can attain up to 70% of $V_0$. Similar qualitative guess can be obtained also from Fig. 5a for the half-spheroidal body. If the spheroid is not permeable ($\kappa_T/\kappa_1 = 0.2$), the region with $V_z < 0$ and $q_{cn} > 0$ is in the right quarter of the spheroid as can be seen from Fig. 5b. More precise calculation of the refraction and convective heat flow anomaly *(Hvoždara, 2005)* will be the subject of a separate paper in preparation.

***Acknowledgments***. The author is grateful to the Slovak Grant Agency VEGA for partial support of the work by means of project No. 2/7008/27.

## References


Arfken G., 1966: Mathematical methods for physicists, Academic Press, London, 1966.

Bear J., Verruijt A., 1987: Modeling Groundwater Flow and Pollution. D. Reidel Publ. Comp., Dordrecht.

Cook K. L., Van Nostrand R. C., 1954: Interpretation of resistivity data over filled sinks. Geophysics, 19, 761–770.

Hvoždara M., 2005: Geothermal anomaly due to a cylindrical obstacle buried in the halfspace with groundwater flow. Contr. Geophys. Geod., **35**, 2, 113–125.

Madelung E., 1957: Die Mathematischen Hilfsmittel des Physikers. Spriger-Verlag, Berlin.

Morse P. M., Feschbach H., 1953: Methods of theoretical physics. McGraw-Hill Comp., New York.

Lebedev N. N., 1963: Special functions and their applications. Fizmatgiz, Moscow (in Russian).

Smythe W. R., 1968: Static and dynamic electricity. McGraw-Hill, New York.

Wait J. R., 1982: Geo-electromagnetism. Academic Press, New York.